SPE 75226

Characterization Of Estuary-Shoreface Type Reservoir Using Outcrop Analogue And Modeling Of Flow Using A Nonuniform Coarsened Grid

Sergio A. Merchán, U. Of Calgary; Sanjay Srinivasan, SPE, U. Of Calgary; Rudi Meyer, U. Of Calgary

Abstract
A methodology for constructing an analogue 3D model for clastic reservoirs in an estuary-shoreface depositional environment using outcrop information is discussed. Such analogue models provide valuable information related to reservoir architecture and rock properties that can be used to model sedimentary structures in the subsurface. A new approach for upscaling high-resolution models using nonuniform coarsened grid is introduced. Simulation results for a viscous dominated flow process show that nonuniform grids yield better results compared to uniform grids.

Introduction
Hydrocarbon accumulations in estuary-shoreface type depositional environment are found at numerous locations worldwide. Complex sub-tidal and inter-tidal estuarine channels and shoreface deposits make these reservoirs extremely heterogeneous and difficult to model based on the information available at a few wells. Developing a detailed, high-resolution analogue model based on extensive outcrop data provides valuable information pertaining to spatial variations in reservoir architecture and rock properties. Information available on analogue models can be used to generate high resolution, stochastic models that are constrained to information such as well data, seismic attribute maps, etc. In order to utilize these equi-probable stochastic models for assessing production performance of the reservoir, a robust technique for upscaling the high-resolution models is necessary.

This paper addresses two important aspects of reservoir characterization: (1) Construction of an analogue model for clastic reservoirs in an estuary-shoreface depositional environment; and, (2) Development and validation of a new approach for upscaling high-resolution reservoir models using a nonuniform coarsened grid.

Analogue models are an important first step towards generating high-resolution stochastic models for reservoirs with complex depositional systems. Outcrops provide valuable information related to reservoir heterogeneity that can be used to model sedimentary structures in the subsurface. The proposal is to utilize outcrops of the upper Cretaceous Virgelle Member of the Milk River Formation in southern Alberta, Canada for developing the analogue model. This was a progradational depositional system representing environments from marine offshore through shoreface and foreshore[1]. The presence of sub-tidal and inter-tidal estuarine channels is a typical feature of such deposits. A consistent methodology for assembling outcrop data available on multiple 2-D sections, into 3D gridded models is presented. The approach integrates permeability and porosity measurements, stratigraphic columns, multiple vertical sections, and facies information to form a deterministic model for the clastic reservoir.

Modern geostatistical reservoir modeling techniques, such as stochastic methods, are routinely used to generate multiple, equally probable models, each optimally constrained to the available data. These models quantify the uncertainty associated with sparsity of information. Unfortunately, these models are often too large and the resulting flow models are extremely *cpu* demanding. Upscaling methods try to reduce the size of these detailed models without loss of accuracy. The proposed algorithm first identifies regions of high connectivity using streamline simulation. The nonuniform coarse-scale grid is then constructed preserving areas with high connectivity. This method preserves the geological and flow characteristics better than uniform upscaling techniques.

Using outcrops for modeling
The evaluation of critical factors associated with estuary-shoreface clastic reservoirs can be improved using data from analogue outcrops where large and small-scale heterogeneities can be studied in more detail. Excellent outcrop conditions allow continuous tracing of sedimentary units over large areas leading to a better understanding of reservoir architecture.

Furthermore, outcrop data can provide detailed information on the geometry and texture of sedimentary bodies and their

internal heterogeneities. Statistical analyses to quantify spatial patterns of heterogeneity are difficult or impossible to perform based on subsurface data.

Outcrop information has been used by other researches for calculating parameters such as vertical permeability[2,3], sand body continuity[4], proportion of channel deposits, sand body width and thickness[5], and for evaluating the importance of internal heterogeneity[6]. Based on outcrops studies, Halvorsen & Hurst [6] showed that core plugs do not resolve important permeability or lithological variations present in many reservoir settings. Models based on core plugs alone tend to undersample the heterogeneity present. Goggin et al[8] showed that statistical measures of variability and spatial correlation and general descriptions of reservoir architecture, are portable between the outcrop and the subsurface in the case of an eolian system. Recently, Jennings[9] presented a statistical analysis of outcrop permeability data for quantifying spatial patterns of petrophysical heterogeneities in carbonates. Ringrose et al[6] used a small outcrop (10m. x 100m.) of fluvial deltaic sandstone to evaluate the importance of internal heterogeneity for a hypothetical waterflooding displacement process.

Several outcrops studies have been undertaken on different sedimentary rocks such as carbonates[9], and sandstone-shale successions corresponding to fluvial-deltaic[10,6], fluvial[11,12], tide-influenced deltaic[13], and eolian[8] depositional environments. Most of these studies involved 2D models with the exception of Ringrose et al[6], who worked with a small 3D model. The study developed by Meyer[1] is one of the few published studies considering shoreface and estuarine channels.

Statistical measures of reservoir heterogeneity inferred from outcrop studies can be applied to actual reservoirs, with similar depositional environment. This implies that spatial patterns in permeability and porosity estimated from outcrops are analogous to those in reservoirs of similar geological type. Several studies have shown that this is an acceptable assumption for clastic deposits. It is to be noted that diagenetic alterations can be significant and may affect the transportability of parameters such as the mean permeability and porosity.

Geologic setting of the Milk River Formation

This research is based on the study by Meyer[1] pertaining to Writing–on-Stone Provincial Park (WOSPP) located about 9 Km north of the international border between Canada and USA. The area spans a rectangular area of 6 Km (west-east) by 4 Km (south-north). The Milk River Formation is subdivided into three members, from base to top:

- The Telegraph Member: Interbedded gray shale and very fine sandstone.
- The Virgelle Member: the subject of this paper.
- The Deadhorse Coulee Member: interbedded gray–brown purple mudstone and light–brown fine to medium-grained cross-bedded sandstones.

Figure 1 illustrates the depositional model for the Virgelle

and Deadhorse Coulee Members at Writing-on-Stone Provincial Park proposed by Meyer.[1] The main features are the east-west trending tidal bars that truncate the middle shoreface and build a subtidal platform at the estuary mouth, and the similarly oriented estuarine meander belt that, as it progrades, erodes tidal bars and scours into the upper middle shoreface.

Lithofacies framework. Meyer[1] identified and described nine (9) lithofacies based primarily on physical and biogenic sedimentary structures. A summary of lithofacies, their characteristics and interpretations of depositional sub-environments is given in Table 1. Based on the various stratigraphic columns three (3) lithofacies associations were defined:

1. Middle shoreface
2. Tide-dominated and wave -dominated upper shoreface
3. Estuarine channels

A muddy supratidal flat deposit, representing the coastal plain or backshore, overlies all three groups. These associations are considered to be typical shoreface end-members, from open marine coast to an adjacent, major estuary.

Middle shoreface. This association is composed of storm-dominated lower-to-middle shoreface deposits at the base (lithofacies 1 and 2, see Table 1) and is truncated sharply by a disconformity that separates it from the overlying upper shoreface/foreshore (Lithofacies 5 and 3b). The lower-to-middle shoreface is 20-25 m thick, coarsening and thickening upward from interbedded very fine-grained sandstone and mudstone, to thick, fine-grained sandstones and rare, very thin mudstone lenses.

Tide-dominated and wave -dominated shoreface. Tidal sand bar deposits of lithofacies 3b overlie the upper middle shoreface separated by a sharp disconformity. Lithofacies 3b corresponds to the zone of subtidal to intertidal sand bars corresponding to an outer estuary. They are regionally extensive with approximately equally significant current directions ESE and WNW. They are interpreted to represent deposition at the mouth of a SE to ESE trending estuary. The tidal sand bar deposits commonly have a thickness of 5-8 m but reach a maximum thickness of 14 m at the south end of the area of study. They occupy the entire interval between the middle shoreface deposits below, and the thick, muddy coastal plain paleosols of lithofacies 7 above. The bars are made-up of crossbeds of Lithofacies 3b, with very rare, thin interbedded mudstone lenses. The wave-influenced upper shoreface/ foreshore sandstones of Lithofacies 5 have a maximum thickness of 8 m. This lithofacies is rare in the study area, exposed in outcrops of only limited lateral extent and with 2-3m thick erosional remnants below channel Lithofacies 3a.

Estuarine channels. Complex estuarine channel deposits are prominent and characteristic of many outcrops at WOSPP. The channels involve lithofacies 3a and 4. Individual channels are about 200-400 m wide, 3-10 m thick and have coalesced to form a meander belt at least 5 km wide at WOSPP. The meandering nature of these channels is well illustrated in

Figure 2, showing the elevation of contours at the truncated top of the middle shoreface. Most of the channels bodies contain both sandy channel bar deposits, as well as muddy, heterolithic, abandoned channel fills (lithofacies 7). A typical channel sequence begins with very thick (1-1.5 m) tabular dunes at the base, grading upwards into 50-80cm-thick 3D-dunes that become progressively smaller and are sharply overlain at the top by current rippled sandstone, often incipiently weathered (*e.g.* mottled, rooted). Other channels appear to be composed entirely of 3D-dunes, large-scale at the bottom, and diminishing in size to 3D current ripples at the top.

Data considered in this study. To generate the model for the Virgelle Member, we have used part of the detailed sedimentologic data collected by Meyer[1], along continuous outcrops within WOSPP and adjacent areas. The salient data comprises the following:

Stratigraphic columns. The columns depict sedimentologic details of the units (middle shoreface, upper shoreface and estuarine channels). They include brief descriptions and lithofacies identification accompanied by rose diagrams of the corresponding current flow indicators and lateral accretion surfaces. A map showing the location of sixty-nine (69) stratigraphic columns is presented in Figure 3.

Contour maps. The contact between upper and lower units (top of the middle shoreface) is in general a regional and well-exposed surface, allowing the contour mapping of this contact. The low number of reliable contacts at the top of the upper unit and the base of the lower unit could not be used to produce tenable contour maps.

Cross Sections: The study by Meyer included three (3) cross sections. Six (6) additional cross-sections were constructed for this study using the outcrop information available on the stratigraphic columns. The location of the nine (9) cross-sections is shown in Figure 3 with corresponding labels. Attention was placed on the elevation of the contacts between middle shoreface/upper shoreface, middle shoreface/estuarine channel and upper shoreface/ estuarine channel. All nine (9) cross-sections were digitized, and examples of three such sections are presented in Figure 4.

Permeability samples. Cylindrical plugs were extracted from subsurface cores and outcrop samples. Permeability values corresponding to 1,573 plugs were available, 783 from cores and 790 from outcrops. Three mutually perpendicular plugs were obtained for each outcrop block: horizontal and parallel to the strike of bedding planes or laminae (HPA), horizontal and perpendicular to the former, sub-parallel or at a shallow angle to bedding (HPE), and vertical, at a high angle to bedding (V). Gas permeabilities were calculated from steady state flow test on 3.81cm (1½-inch) plugs and a confining pressure of 2.8 MPa (400 psia) needed to seal the sample and prevent bypass. Large sample sets from lithofacies 2,3 and 5 were available; but current- and wave-rippled lithofacies 6 (3 plugs) and 8 (none) were both too thin and break too easily across fine-scale laminae, to allow plugs to be drilled. Table 2 shows the distribution of permeabilities by lithofacies.

Core Samples: The cores were recovered from four (4) wells, drilled along the northern margin of the Milk River valley. These cores provided samples for closely spaced permeability tests and accounted for small-scale physical and biogenic structures on fresh rock surfaces, not visible on weathered outcrop surfaces. Figure 5 shows the vertical distribution of horizontal permeability for the four wells.

Outcrop Samples. To obtain outcrop samples, large blocks of about 3,000 cm^3 in volume (ideally 20 x 15 x 10 cm) were extracted from vertical sections at intervals approximating 1-2m.

Porosity. One hundred and eighty-one (181) plugs were selected for porosity measurement. Porosity (ϕ) was calculated at zero stress based on bulk volume determined by mercury displacement, and grain volume measured in a U.S.B.M. modified Boyle's Law apparatus using helium gas. The uncertainty of ϕ is estimated at ± 0.5 %.

Transforming outcrop data into gridded models

The methodology for constructing the 3-D analogue model, that correctly honors the data available and the stratigraphic geology and interpretation, consisted of the following steps.

Definition of genetic units and statistical analysis. Lithofacies were grouped into genetic units, based on lithofacies description, successions and representing sedimentation in different depositional environments. The final genetic units are middle shoreface, upper shoreface and estuarine channels. Each genetic unit and its petrophysical data were analyzed using descriptive statistical methods: mean, variances, correlation coefficients, histograms, cross-plots and semivariograms[15,16,17]. Average petrophysical properties are summarized for genetic units in Table 3. In a general sense, the middle shoreface exhibits the lowest average permeability and the estuarine channel the highest average permeability with a higher variance.

Construction of the stratigraphic framework. This phase is focussed on reproducing the architecture and the large-scale trends of the genetic units. The elevation points for the middle shoreface and the (9) cross sections were digitized. First, the elevation at the top of the middle shoreface was modeled. Then the thicknesses of the middle shoreface, upper shoreface and estuarine channel were interpolated from the information available on cross-sections. In order to obtain the top surfaces of the upper shoreface and the estuarine channel, the thicknesses of these genetic units were added to the top surface of the middle shoreface. The base of the middle shoreface was obtained by substracting the middle shoreface thickness. This approach ensures that no negative values for thicknesses are obtained. The elevation at the top of the middle shoreface and thickness of each genetic unit was interpolated using sequential gaussian (**sgsim**). The output data was processed to generate numerous cross-sections in north-south and east-west directions. These interpolated cross-

sections were analyzed for consistency with the depositional model. The final stratigraphic model utilizes additional control points that were introduced to ensure that the spatial correlation, shape of geological features and lithofacies sucessions were accurately represented by the output data. Special attention was placed on features such as the channel defined in the north part of the study area and the tidal bar in the south; see Figure 2. In general the amount of control points added were between 1- 10 % of the original data, depending on the surface. It could be argued that stochastic simulation techniques such as **sgsim** would provide a non-deterministic rendition of the surfaces. However the generated surfaces exhibit little variation in the general pattern of elevation and thickness. Some variations were observed mainly in the southeast section of the model, due to the lack of data in that part of the model. Figure 6 shows a view of surfaces corresponding to the top of the middle shoreface and the upper shoreface, generated considering a 100x100 grid. Estimations of volume between surfaces showed proportions of genetic units as follows:

- Middle shoreface   69.0 %
- Upper shoreface   8.4 %
- Estuarine channels   21. 6%

Assigning physical properties. Subsequent to the construction of the surfaces, petrohysical properties were assigned to the genetic units bound by the surfaces. In order to accomplish this, the coordinates of the permeability and porosity measurements were stratigraphically transformed. All measurements served as hard data.

Horizontal permeability. In the vertical direction the semivariogram of horizotal permeability was clearly inferred using the high density of available information given by the cored wells. However, in the horizontal direction the semivariogram cannot be reliably inferred, due to the low density of data. The horizontal variogram range was identified to the range of the indicator variogram inferred on the previously constructed model for genetic units.

Sequential Gaussian Simulation was utilized to generate models for the horizontal permeability corresponding to each genetic unit. Ultimately, the three genetic units were merged to obtain the final model. The final model has a total of 500,000 cells (100x100x50); cell dimensions are 60m x 40m in the x and y direction respectively, and approximately 0.8 m in the vertical direction.

Vertical permeability and porosity. Sequential Gaussian co-simulation with horizontal permability as secondary variable was utilized to generate the vertical permeability model and the porosity model.

Again, multiple cross-sections and vertical transects of the permeability field and porosity were analyzed and checked for consistency with the prior geological model. An attempt was made to retain important features such as low and high permeability streaks. Figure 7 shows the final analogue model and some cross sections illustrating the location of the channel and extreme permeability regions that honors the data available and the stratigraphic geology and interpretation.

The construction of the above model requires stochastic simulation and interpolation. Stochastic simulation permits reproduction of spatial variability and hence, was the tool of choice for generating the 3D analogue model. It is believed that the presence of high density of information and the extensive and iterative verification process adopted renders the resultant analogue as close as possible to the prior geological vision of the depositional system.

Upscaling

Upscaling is a procedure that transforms a detailed geological model to a coarse–grid simulation model such that the flow behaviour in the two systems are similar. Upscaling is required because fine scale flow simulation of multiple high-resolution models can be *cpu* expensive. Any upscaling procedure involves basically two steps, (1) gridding, to capture the general geologic features, and (2) averaging or estimation of properties, to preserve the local geologic details. Different authors[18-23] have stated the advantages and disadvantages of the different upscaling procedures and proposed new methodologies. Despite the numerous upscaling methods reported in literature, efficient and accurate estimation of effective rock properties of coarse scale from geological data at fine scale remains an active area of research.

Uniform vs. nonuniform grid. In uniform gridding methods, the coarse-grid cell boundaries of the permeability field are independently and somewhat arbitrarily defined, and then a scale-up method is applied to the permeabilities within the boundaries of each coarse-grid cell. If the coarse-grid cell contains extreme values such as large flow barriers and/or high permeability streaks, uniform grid does not give accurate results. Nonuniform grids that preserve the structure of permeability extreme values have been shown to give more accurate results. Durlofsky[18,21,22] developed a method for nonuniform coarsening of the original detailed description, with finer resolution in potentially high flux regions. The high velocity regions are estimated through single-phase flow calculations with the actual well locations. These regions are modeled in detail, using a fine scale permeability description. In regions away from wells, effective properties on a coarse grid are assigned using a general technique based on homogenization theory. Li[20] present a method referred to as global scale-up, which uses a moving window to detect boundaries of regions with large permeability variance and then construct a coarse-scale grid. Their method attempts to maintain the variance and the spatial correlation within the entire permeability field. Panda[19] applied wavelet transforms to one-dimensional and two dimensional permeability data to determine the location of the layer boundaries and other discontinuities and construct a nonuniform grid.

Proposed Approach. The proposed approach is based on non-uniform gridding of the reservoir with finer grids in regions of greater heterogeneity and coarser grids in more homogeneous regions. The connectivity characteristics of different regions are determined by performing streamline

flow simulation. In order to render the non-uniform grid process independent (boundary condition), multiple streamline simulations are performed with a combination of injector/producer locations.

Eleven cases were run, with one injector and one producer in each case. In order to speed up the calculation procedure, the layer with the highest variance of permeability was selected and 2-D tracer simulations were performed corresponding to different well locations on that layer.

Tracer simulations provide information about the location of the streamlines and time of flight. Thus, it is possible to estimate the number of streamlines crossing each fine grid cell corresponding to each injection-production case. Each block is coded one (1) if a streamline intersects it, or zero (0) otherwise. The probability that a block is intersected by a streamline over a combination of injectors and producers is computed. The probability is corrected to reduce the effect of the high density of streamlines around the injector and producer well. This was done by multiplying the probability with a value K/(d*TOF), where k is the permeability of the block, d is the distance from the well to the block along the streamline and TOF is the time of flight along the streamline to the block location. The resultant values are normalized so as to range from 0 to 1.

Nonuniform coarse blocks are obtained by aggregating fine cells such that the variance of probability within each coarse block is minimized. The map of probabilities contains information about the high and low permeability values and their connectivity. The algorithm utilizes a 2-D window to estimate the variance of the probability of streamlines considering a variety of probable coarse block shapes. These blocks range in size with the biggest of 16x4 or 4x16 and the smallest of 2x2. All intermediate combinations are tried and only those with low variance are kept. An iterative procedure is used to accept and reject a possible coarse block to arrive at a final combination with the required number of blocks.

The algorithm for constructing the non-uniform grids utilizes as input the fine scale porosity and permeability field and the desired number of coarsened blocks. The map of corrected probabilities and the non-uniform grid are the outputs. Traditional averaging techniques (arithmetic, geometric and harmonic) were utilized to estimate block equivalent properties. Volume weighted arithmetic average is used for porosity. The output data consists of files with definition of coarse cells (block corners) and upscaled property ready for flow simulation. In the case of 3-D flow simulations, the grid established for this highest-variance layer is applied to all other layers.

Flow simulation. The applicability of the upscaling procedure was tested on one 2-D layer of the analogue model described in the previous sections. A waterflooding scenario with three (3) injector wells and (6) producer wells was simulated. The fine grid model comprised of 100 x 100 cells. The fine model was scaled up in two different ways: a uniform 25x25 coarse grid, and a non-uniform coarsened grid comprising of 625 cells. A single set of relative permeability curves was assumed for the entire reservoir. For both coarsened models, effective block permeabilities were computed using different averaging techniques to compare the effect of averaging on the type of grid selected. The probability map obtained after tracer simulations is shown in Figure 8. The map does not show any undue influence of the injectors or producers. The permeability fields corresponding to the uniform and nonuniform grid are shown in Figure 9. They reflect the permeability heterogeneities observed in the fine scale model also shown in Figure 9.

Figure 10 shows the water saturation map corresponding to the fine grid, uniform coarse grid and the non-uniform coarsened grid. Comparisons on the basis of well and field performances are presented in Figure 11. All flow simulations were run on a commercial simulator. Results show that for the conditions of this problem, viscous dominated flow, non-uniform coarsened grids are superior in performance to uniform coarsened grids. This result is true even when the effective properties of the uniformly coarsened blocks are estimated using a flow-based upscaling technique, while the nonuniform block properties were estimated using arithmetic/harmonic averages. Nonuniform gridding results in better reproduction of the field cumulative oil production and well water cut and breakthrough time behavior. These results are consistent with previous studies by Durlofsky[18,22] and Li[20]. Furthermore, differences between the results corresponding to arithmetic and harmonic averages for block properties are reduced for the non-uniform coarsened grid.

Discussion and Conclusions

The proposed nonuniform gridding approach preserves the continuity of the permeability extremes. This results in better reproduction of the flow behavior of the reservoir and better predictions for key characteristics such as breakthrough time. Although, there is an initial cost associated with generating the map of probabilities quantifying the influence of different reservoir regions on flow, the overall cost of flow simulation and performance prediction is significantly reduced. The non-uniform coarsened grid is process independent and can be used to simulate flow corresponding to arbitrary well configurations.

The paper also presents a methodology for constructing an analogue model for clastic reservoirs in an estuary-shoreface depositional environment using outcrop information. Such an analogue model provides valuable, high-resolution information related to reservoir architecture and rock properties (permeability and porosity) that can be used to model sedimentary structures in the subsurface.

Although several important aspects of analogue model construction and upscaling for flow simulation are discussed in this paper, some important issues warrant further research. The methodology for non-uniform upscaling has been demonstrated for a single layer case, corresponding to viscous-dominated flow conditions. It is quite likely that in multilayered reservoirs and gravity dominated flow conditions, the assumption that the non-uniform coarsened grid corresponding to the layer with the maximum variance

applies to all layers may be invalid. A refinement to the grid coarsening approach considering a variety of 3-D templates may be necessary. Assigning realistic effective permeabilities to the non-uniform grid blocks is also non-trivial. A power average technique with locally varying power exponent ω may be optimal for that purpose. A procedure for calibrating such power averages is currently being developed.

Patterns of continuity exhibited by geological features such as channels can be captured using multiple point correlation functions. These functions can be inferred on the analogue model. A multiple point statistics based approach to simulate realistic reservoir models for similar depositional system will be attempted.

Acknowledgements

References

1. Meyer, R., Sedimentology, Petrology And Permeability Characterization Of The Upper Cretaceous Virgelle Member, Milk River Formation, Writing-On-Stone Provincial Park, Alberta, Canada. PhD dissertation, University of Calgary, AB. Canada, 1998.
2. Haldorsen, H.H. and Lake, W., A new approach to shale management in field-scale models. SPE journal, (August), p. 442-452, 1984.
3. Begg, S.H., and King, P.R. Modelling the effects of shale on reservoir performance: calculation of effective vertical permeability. SPE 13529, 1985.
4. Clementsen, R., Hurst, A, Knarud, R. and More, H., A computer program for evaluation of fluvial reservoirs. In: North Sea oil and Gas reservoirs –II (Ed. By A.T. Buller, E. Berg, O. Hjelmeland, J. Kleppe, O. Torsaeter and J.O. Aesen), p. 373-385, Graham and Trotman, London, 1990.
5. Bridge, J.S. and Mackey S.D. , A theoretical study of fluvial sandstone body dimensions. In: The geological modeling of Hydrocarbon reservoirs and outcrop analogues. Edited by Stephen S. Flint and Ian D. Bryant. Special publication No. 15 of the international association of sedimentologists. Blackwell scientific publications, 1993.
6. Ringrose, P. Et al., The Ardross Reservoir gridblock analogue: Sedimentology, statistical representativity and flow upscaling. In: R. Schatzinger and J. Jordan, eds., Reservoir Characterization-Recent advances, AAPG Memoir 71,p. 265-276, 1999
7. Halvorsen, C. and Hurst, A, Principles, practice and applications of laboratory minipermeametry. In: Advances in core evaluation: Accuracy and precision in reserves estimation (EUROCAS I)(Ed. By P.F. Worthington, p. 521-549. Gordon &Breach, London, 1990.
8. Goggin, D.J. et al., Permeability transects of eolian sands and their use in generating Random permeability fields. SPE formation evaluation. March, p.7-16, 1992.
9. Jennings, J. W., 2000, Spatial statistics of permeability data from carbonate outcrops of West Texas and New Mexico: implications for improved reservoir modeling. Report of investigation No 258. The University of Texas at Austin.
10. White, C. D., and Barton, M. D., Comparison of the recovery behavior of contrasting reservoir analogues in the Ferron sandstone using outcrop studies and numerical simulation. Report of investigation No 249, The University of Texas at Austin.,1998.
11. Jacobsen, T., and Rendall, H., Permeability patterns in some fluvial sandstones. An outcrop study from Yorkshire, North East, England. Reservoir Characterization II Academic Press. Lake, L.W. et al, p.315-337, 1991.
12. Cuevas, G. and Martinius, A. W., Outcrop database for geological characterization of fluvial reservoirs: An example from distal fluvial fan deposits in the Loranca basin, Spain. FromNorth, C.P.& Prosser, D.J. Characterization of fluvial and aeolian reservoirs. Geologic Society special publication No 73. p. 79-94, 1993.
13. Willis, B. J. and White, C., Quantitative Outcrop data for flow simulation. Journal of Sedimentary Research, vol. l70, No 4, July, p. 788-802, 2000
14. Lewis, J.J.M., Outcrop-derived quantitative models of permeability heterogeneity for generically different sand bodies. SPE 18153 presented at the 63rd annual conference and exhibition of the SPE 1988.
15. Deutsh, C.V. and Journel, A.G., **GSLIB: Geostatistical Software Library and User's Guide**, Oxford University Press, Inc., Oxford, 1998.
16. Isaaks, E.H. and Srivastava R.M., **An Introduction to Applied Geostatistics**, Oxford University Press, Inc., Oxford, 1989.
17. Journel, A.G. and Huijbregts, C. **Mining Geostatistics**, Academic Press, New York, 1978.
18. L.J. Durlofsky. 1991. Numerical calculation of equivalent grid block permeability tensor for heterogeneous porous media. Water resources research 27(5): 699-708,1991.
19. Panda, M., Mosher, C. and Chopra, A. Application of wavelet transforms to reservoir data analysis and scaling. SPE 36516. Paper presented at the Annual Technical Conference and exhibition, Denver, Colorado, October 1996.
20. Li, D., A.S. Cullick, and L.W. Lake. Global scale-up of reservoirs model permeability with local grid refinement. J. Pet. Sci. and Eng., 14:1-13,1995.
21. Durlofsky, L.J., Jones, R.C, and Milliken W.J. " A new method for the upscale up of displacement processes in heterogeneous reservoir. Proceedings of the 4th European conference on the mathematics of oil recovery, Roros, Norway, June 1994.
22. Durlofsky, L.J., Behrens, R.A., Jones, R.C. and Bernath, A. Scale Up of heterogeneous three dimensional reservoir descriptions. SPE 30709, SPE Journal, September 1996.
23. Lee, S.H., Durlofsky, L.J., Finite Difference Simulation of geologically complex reservoirs with tensor permeabilities. SPERE Dec., 1998.
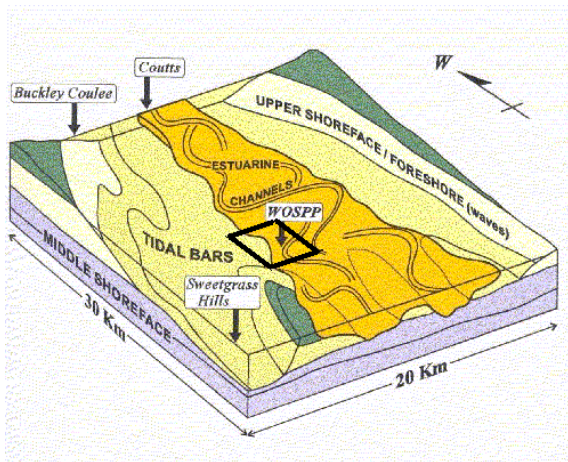
Figure 1 - Schematic block diagram illustrating the depositional model proposed for the Virgelle and Deadhorse Coulee Members at Writing-on-Stone Provincial Park; the rectangle represent the area studied in this paper, from Meyer[1]
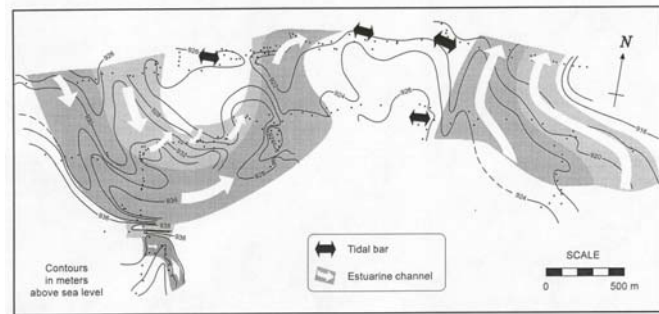
Figure 2 – Structure contours of the top of the middle shoreface showing the curving, relatively steep outlines of the erosional base of the meandering estuarine channel, and broad, sub-horizontal topography at the base of the tidal bars. Large black and white arrows point in the predominant current direction of tidal bars and estuarine channel respectively, from Meyer.[1]
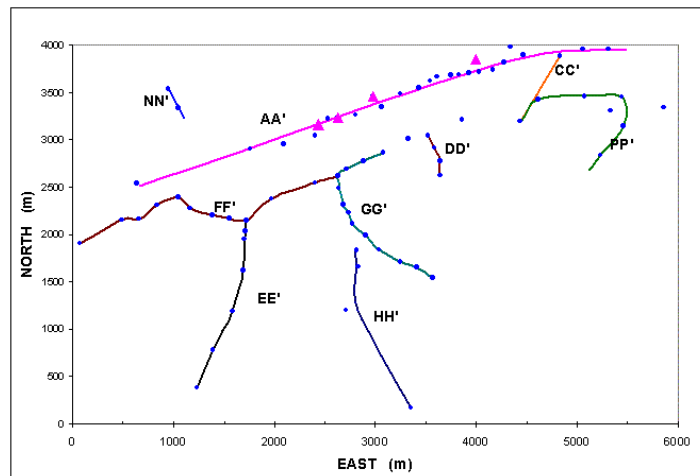
Figure 3 - Areal map showing the location of the stratigraphic columns (points), cross-sections (lines), and wells (triangles) within Writing-on-stone Provincial Park, WOSPP.   The area of study covered 6 Km x 4 Km.
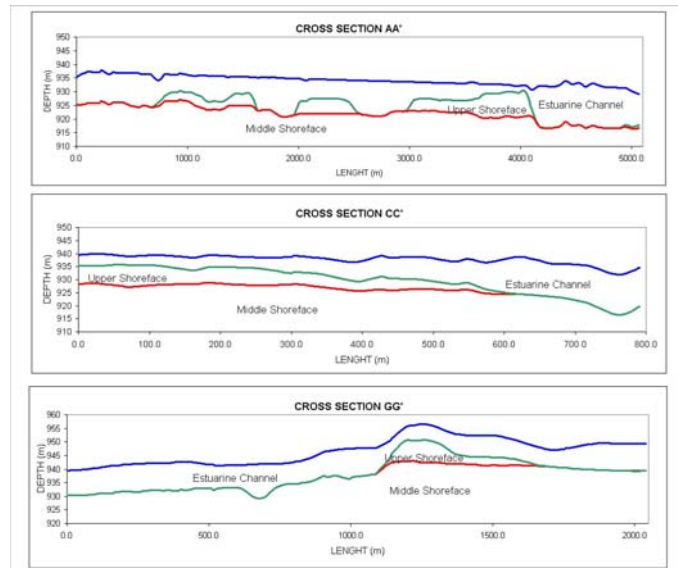
Figure 4 - Example of cross sections digitized (AA', CC' and GG'). In sections like shown in AA' (top) the estuarine channel has eroded totally the upper shoreface in some areas, therefore it is not present. The lines correspond to the elevation of the contacts middle shoreface, upper shoreface and estuarine channel.
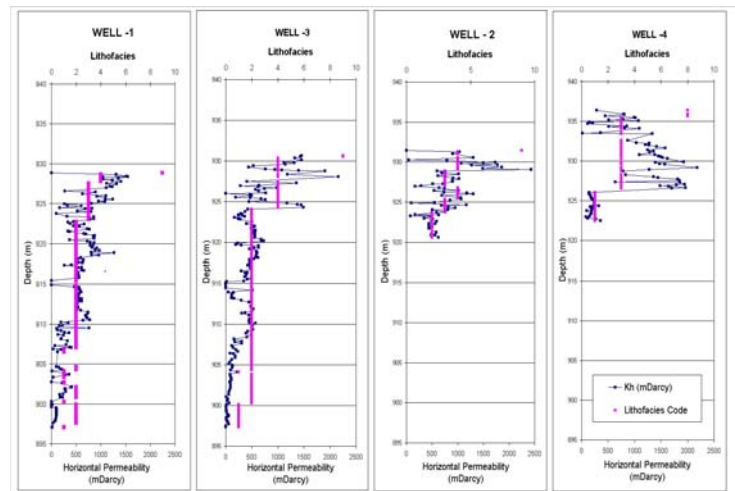
Figure 5 - Vertical trends of horizontal permeability for the four wells drilled in Meyer[1] study.   The straight line corresponds to the lithofacies code according to table 1. Two (2) of the wells, numbers 1 and 3, are separated by about 1 km and cored from near the top of the Virgelle Member to very close to-or within the transition to the underlying Telegraph Creek Member. The other two wells, numbers 2 and 4, only penetrated the upper unit to a few meters below the contact with the lower unit. Well #2 is located approximately equidistant from the others, whereas well #4 is placed only 50m away from well #3 illustrating the local variability within the same channel-form cutting several meters into the lower unit
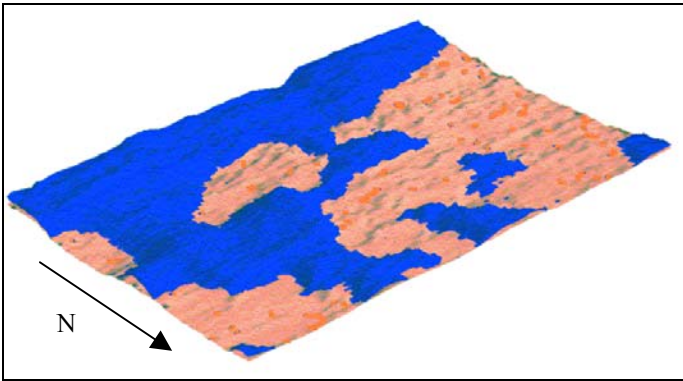
Figure 6 – Projection of the surfaces corresponding to the top of the middle shoreface (light) and the upper shoreface (dark), generated considering a 100x100 grid (6000 m x 4000m). Note the east west trending tidal bar (south) and the similarly oriented estuarine meander belt. The vertical scale has been exagerated 10 times.
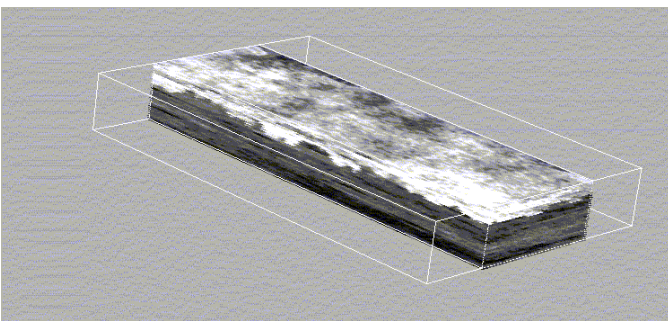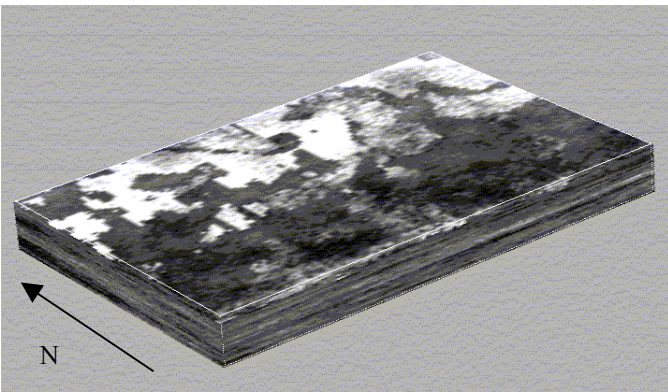
Figure 7 - 3D projections of the horizontal permeability field of the analogue model (stratigraphically transformed). Light areas correspond to high permeability values. Lower figure is a section of the same model showing the channels close to the top. The vertical scale has been exagerated 10 times.
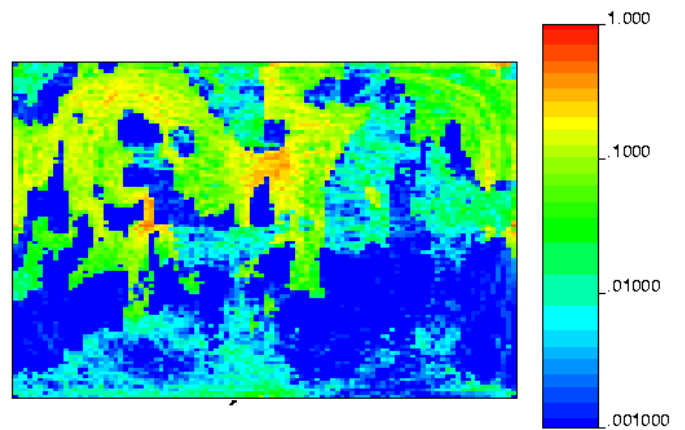
Figure 8 – Map of probability of streamlines obtained after several streamline simulation.

.
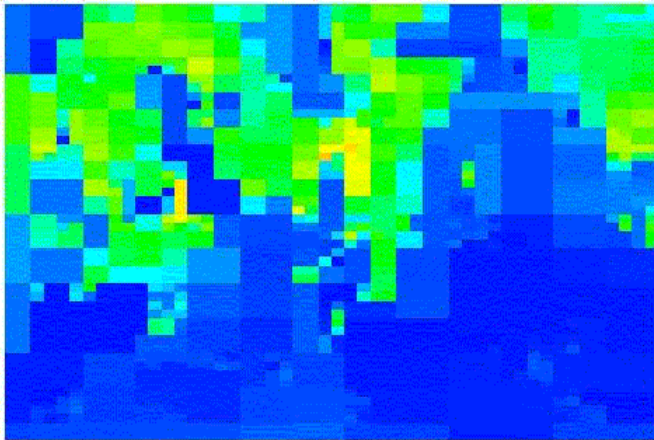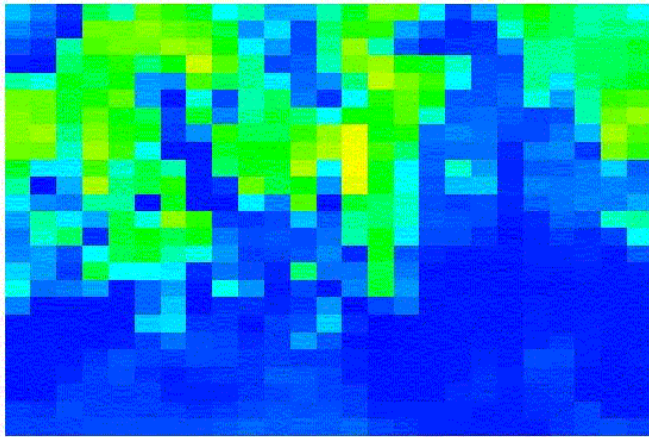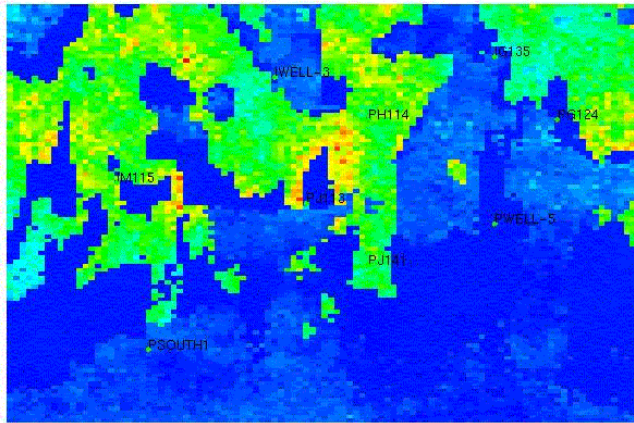
Figure 9 - Comparison of permeability scale-up using the uniform and the non-uniform approach proposed. Top: the fine grid with 100x100 cells; middle: uniformly upscaled with 25x25 using arithymetic average; lower: the non-uniform grid with 625 cells. Lighter regions indicate higher permeability. We selected the most heterogeneous layer for comparisons.
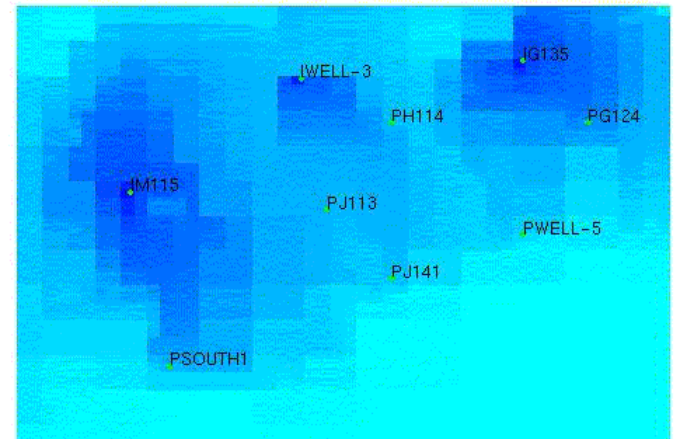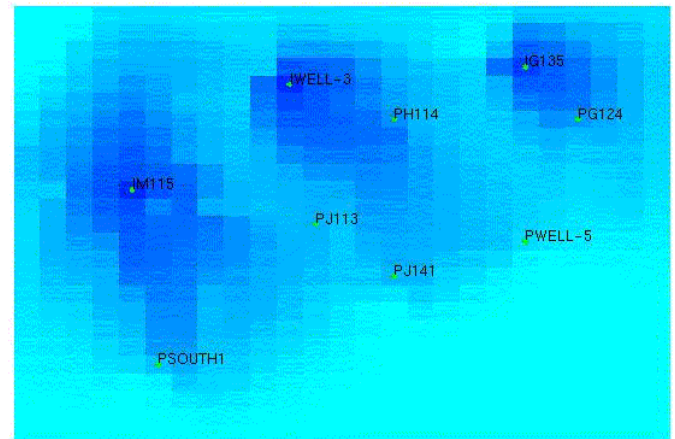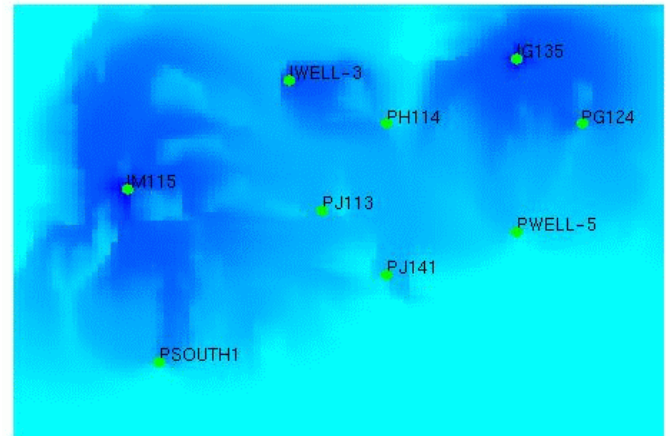
Figure 10 - Water saturation profiles after 5 years of water injection for the fine, uniform and the non-uniform upscaled grid. Darker areas correspond to higher saturation values.
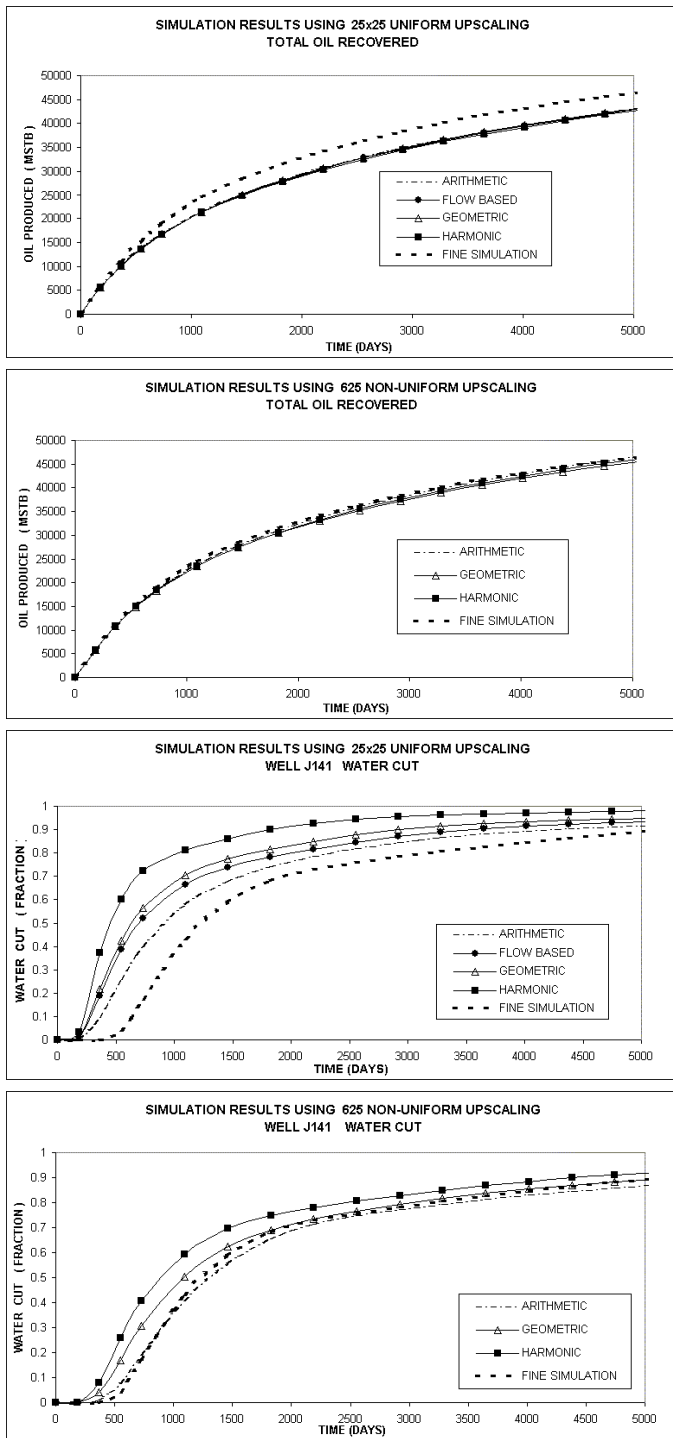
Figure 11 - Comparison of cumulative oil produced for the total field and water cut behavior for a producer well (J141). The results are shown for different averages and corresponding to different grids.

Lithofacies Number	Interpretation.	Description	Genetic unit
1	Offshore to lower shoreface	Burrowed, interbedded very fine grained, wave rippled and thinly laminated hummocky cross-bedded grey sandstone and dark grey mudstone	Considered Lower boundary
2	Middle shoreface	Medium to thickly bedded, laminated, very fine to fine grained, light brown, hummocky and swaley cross-bedded sandstone	Middle Shoreface
3a	Estuarine channel	Fine to coarse grained, medium-to very thickly bedded, 3D and 2D cross-bedded sandstone	Estuarine Channel
3b	Subtidal/intertidal distal tidal bar	Fine to medium grained, medium-to very thickly bedded, "herringbone" cross-bedded sandstone	Upper shoreface
4	Estuarine channel basal dunes	Subrounded to angular, pebble-to-boulder-sized mudstone-and sandstone-clast conglomerate	Estuarine Channel
5	Wave-influenced upper shoreface to foreshore	Fine to medium grained, planar parallel-laminated and low- angle 3D cross-bedded sandstone	Upper shoreface
6	Estuarine channel margin, abandoned channels, coastal flat	Fine-grained, very thin to thinly bedded, laminated current rippled sandstone	Estuarine Channel
7	HIS, abandoned channel fill, coastal flat paleosols	Grey-brown-black, laminated mudstone and shale, and varicoloured, pedoturbated mudstone	Considered Upper boundary
8	Upper shoreface	Fine-grained, very thin to thinly-bedded, wave rippled sandstone	Upper shoreface
9	Intertidal to supratidal estuarine flat	Paleo-weathered sandstone	Considered Upper boundary

Table 1 - Summary of lithofacies characteristics of the Virgelle member at Writing-on-stone Provincial Park.

Lithofacies -ID	Number of samples	
	Kh	Kv
1	31	14
2	549	303
3a	853	410
3b	201	101
4	24	13
5	58	24
6	2	1
8	NA	NA
9	28	16

Table 2 - Distribution of horizontal and vertical samples by lithofacies. Lithofacies 6 (3 plugs) and 8 (none) are both too thin and break too easily across fine-scale laminae, to enable plugs to be drilled.

Genetic units lithofacies	Mean values		
	Kh	Kv	Porosity
	mD	mD	%
Middle Shoreface 2	429.88	359.84	26.36
Upper Shoreface 3b, 5, 8	1011.49	705.53	27.05
Estuarine Channel 3a, 4, 6	1312.31	1018.66	27.95

Table 3 - Average petrophysical properties for each genetic unit.